Journal of Power Sources 245 (2014) 475–481

Contents lists available at SciVerse ScienceDirect

Journal of Power Sources

journal homepage: www.elsevier.com/locate/jpowsour

Synthesis and characterization of polyaniline and polyaniline – Carbon nanotubes nanostructures for electrochemical supercapacitors

Marcela A. Bavio [a,b], Gerardo G. Acosta [a,b], Teresita Kessler [a,c,*]

[a] Facultad de Ingeniería, INTELYMEC-CIFICEN, UNCPBA, Avda. del Valle 5737, Olavarría, Buenos Aires, Argentina
[b] CONICET, Av. Rivadavia 1917, C1033AAJ, Ciudad Autónoma de Buenos Aires, Argentina
[c] CICPBA, Calle 526 entre 10 y 11, 1900 La Plata, Argentina

HIGHLIGHTS

- PANI and PANI–CNT nanostructures were prepared by a self-organization method.
- Nanoparticles and nanotubes were developed at room temperature.
- PANI–CNT nanocomposites displayed improved capacitive properties in acid solution.

GRAPHICAL ABSTRACT

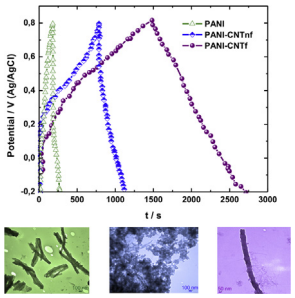

ARTICLE INFO

Article history:
Received 19 April 2013
Received in revised form
17 June 2013
Accepted 20 June 2013
Available online 29 June 2013

Keywords:
Polyaniline nanotubes
Nanocomposites
Carbon nanotubes
Supercapacitors

ABSTRACT

Nanostructures of polyaniline (PANI) and PANI with embedded carbon nanotubes (CNT) were synthesized through a chemical method of self-organization. An oxidative polymerization process was performed in the monomer acid solution with the presence of a surfactant and the addition of multi-walled CNT. The CNT were added with and without pretreatment, CNTf and CNTnf, respectively. Furthermore, ammonium persulfate and sodium dodecyl sulfate were incorporated to the reaction solution as dispersant and oxidizing agents, respectively. Different nanostructures such as nanoparticles or nanotubes were obtained depending on the CNT added, and characterized by scanning electron microscopy, transmission electron microscopy, UV–vis spectroscopy, infrared spectroscopy and electrochemical techniques. Spectroscopy results showed variations in the observed bands of the synthetized nanostructures attributed to changes in the molecular structures, to the state of doped PANI reached during polymerization and to the stabilization of these links by hydrogen bridge interactions. PANI and PANI–CNT composites were evaluated by electrochemical techniques to test their behavior in relation to supercapacitors properties. PANI–CNTf nanocomposites displayed improved capacitive properties in H_2SO_4 solutions, namely 1744 F g^{-1}at 2 A g^{-1}. Also, the specific capacitance was strongly influenced by the developed morphologies. These characteristics point to their feasible application as supercapacitors materials.

1. Introduction

In recent years, materials with special characteristics have been developed in relation to technological devices specially applied to environmental care and clean energy production, such as polluting gas sensors, fuel cells, solar cells, electrochemical capacitors [1–4].

* Corresponding author. Facultad de Ingeniería, INTELYMEC-CIFICEN, UNCPBA, Avda. del Valle 5737, Olavarría, Buenos Aires, Argentina.
E-mail address: tkessler@fio.unicen.edu.ar (T. Kessler).

0378-7753/$ – see front matter © 2013 Elsevier B.V. All rights reserved.
http://dx.doi.org/10.1016/j.jpowsour.2013.06.119

For the latter case, these systems store electrical energy through double-layer charging steps, faradaic processes or a combination of both ways. The whole process is highly reversible and the charge/discharge cycle can be repeated over and over again, virtually without limit.

The electrochemical capacitors or supercapacitors differ from the conventional dielectric capacitors in their special energy storage modes leading to significantly higher values in energy density (usage life after one charge) and in power density (rate of discharge) terms [1,3].

From practical and technological points of view, electrochemical capacitors are robust devices that can improve the effectiveness of battery-based systems by decreasing the number of required batteries and by reducing the frequency of their replacement. The carbon family offers a number of components to be applied in supercapacitors; they are, among others, activated carbon, carbon black, carbon nanotubes (CNT) and graphene. In particular, CNT are considered as promising materials for catalyst supports in fuel cell electrodes, storing hydrogen devices, sensors and as supercapacitors, due to their thermal stability, the chemical and mechanical properties, their good conductivity and high surface area [2,5–7].

A route to enhance the capacitance of a material is adding specific substances providing fast pseudo-faradaic redox reactions. Thus, ruthenium oxide and conductive polymers such as polyaniline, polypyrrole, polythiophene, or their derivatives are suitable materials to synthetize composites to provide higher capacitance [2,8,9].

Polyaniline (PANI) is one of the most extensively studied conducting polymers, because it can be obtained in relatively simple and not expensive ways, it is stable at room temperature and it is an ionic-electronic conductor in a wide potential range [11–13]. There are different chemical and electrochemical methods of synthesis. In this respect, the electrochemical techniques are applied to obtain high purity polymer samples, while the chemical routes offer the possibility to produce easily a large amount of substance. The polymeric nanostructures show an improved performance in technological applications, due to their unique characteristics derived from the nanoscale size; among others, high electrical conductivity, large specific surface, a mixed ionic-electronic conductivity mechanism and a high discharge capacity to mass ratio. Methods of hard and soft templates can be used for the preparation of conducting polymer nanostructures. In this respect, the polymerization using microemulsions is considered the most promising route because it is a fast and easy way to prepare PANI nanostructures in large scale and at low cost compared to the conventional electrochemical methods [4].

The development of composite materials based on conducting polymers and carbon nanotubes is today one of the main research interests due to the very different properties that can be profited in useful devices [8,14,15]. In this paper, different PANI–CNT nanostructures were prepared by a chemical method of synthesis starting from the monomer solution with added carbon nanotubes, both pretreated and as-received ones. The structure and morphology of the obtained nanostructures were analyzed by UV–vis, FTIR, SEM and TEM. The electrochemical capacitance performances of the developed and chemically characterized nanostructures were investigated in acid solution showing an outstanding behavior.

2. Experimental

2.1. Synthesis of nanostructures of PANI and PANI–CNT

PANI nanostructures were chemically synthesized from a dispersion prepared with 0.045 g of aniline, 0.30 mL of 0.25 M HCl and 0.005 g of sodium dodecyl sulfate (SDS) in 18 mL of distilled water under constant magnetic stirring at room temperature (25 °C) for 20 min. Then, 2 mL of 0.24 M ammonium persulfate (APS) was added to the initial mixture. The resulting dispersion was stirred violently for half a minute. The polymerization process was carried out for 24 h at 25 °C without agitation. The obtained precipitate was filtered and washed until the filtrate solution became colorless. Finally, the residue was dried for 24 h at 60 °C.

PANI–CNT nanostructures were synthetized applying the same procedure with the addition of 0.1 mg mL^{-1} of either functionalized carbon nanotubes (CNTf) or non-functionalized carbon nanotubes (CNTnf) to the initial aqueous dispersion.

The non-functionalized carbon nanotubes (CNTnf) were multiwalled carbon nanotubes used as received. CNTf were obtained after applying an oxidizing pre-treatment in 2.2 M nitric acid to commercially available CNT. The amount of CNT was 0.85 mg mL^{-1} and the suspension was kept at room temperature for 1 h [16]. Then, the preparation was stirred using an ultrasonic bath for 30 min and kept at room temperature for 20 h. Afterward, it was filtered and washed with abundant distilled water to achieve neutral pH in the filtrate solution. Finally, the treated carbon nanotubes were dried at 37 °C for 2 h.

2.2. Characterization methods

Various physicochemical techniques were applied to characterize the prepared nanostructures. Scanning electron microscopy (SEM) images were obtained with a scanning electron microscope Jeol JSM-6460LV and the transmission electron microscopy (TEM) micrographs with a JEOL model 100CX operated at 100 kV. The TEM images were processed with Image J to determine the particle size.

FTIR spectra were recorded between 4000 and 400 cm^{-1} using a Nicolet, Magna 500 (250–4000 cm^{-1}) equipment with CsI optics.

UV–vis spectra were obtained for different samples in aqueous solution, using a spectrophotometer UV-1800 PC MAPADA in the 250–900 nm range.

2.3. Preparation of electrodes and electrochemical measurements

The working electrode was assembled as follows. Firstly, PANI and PANI–CNT nanostructures were scattered in pure isopropanol; then, a suitable amount of Nafion solution was added. Afterward, the dispersion was stirred using an ultrasonic bath for 5 min. The suspension was transferred with a micropipette on a mirror-polished glassy-carbon electrode. The Nafion content in the final mixture was 5 wt % and the amount of PANI or PANI–CNT nanostructures was 0.2 mg cm^{-2}.

Cyclic voltammetry and galvanostatic charge/discharge measurements were used to study the capacitive behavior of the nanocomposite materials. Runs were carried out in the 0.0–1.0 V (vs. RHE) voltage range in 0.5 M H_2SO_4. I/V profiles were obtained at varying the scan rates from 10 to 100 mV s^{-1}. The galvanostatic charge/discharge curves were recorded at different current density values in the 2–100 A g^{-1} range.

All electrochemical experiments were performed using EG&G PAR Model 362 potentiostat/galvanostat connected to a three-electrode cell thermostatized at 25 °C. The counter electrode was a large Pt sheet and the reference electrode was a Ag/AgCl (sat.) electrode.

3. Results and discussion

3.1. SEM and TEM characterization

Fig. 1 shows micrographs of different PANI and PANI–CNT structures to contribute to clarify the morphology influence in the

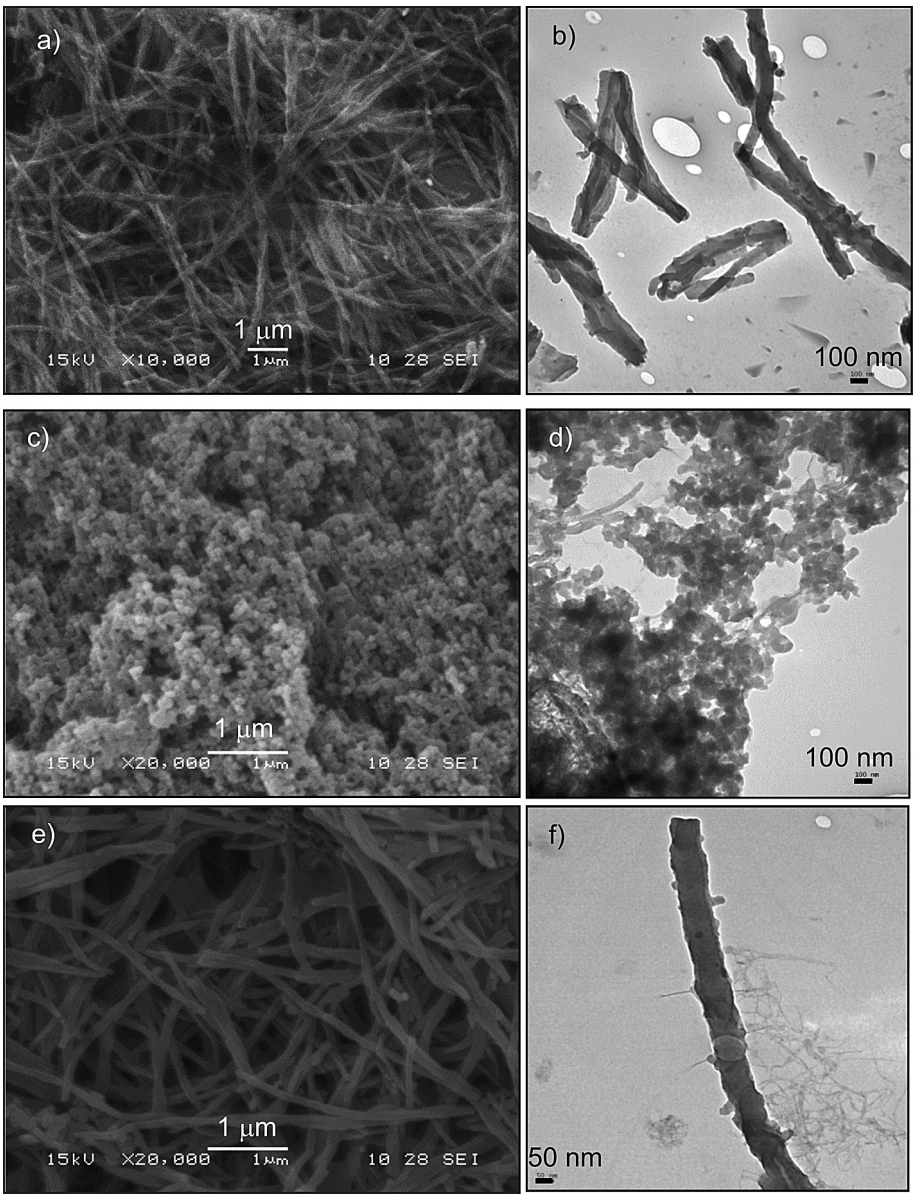

Fig. 1. SEM and TEM images of a,b) PANI, c,d) PANI–CNTnf and e,f) PANI–CNTf nanostructures.

capacitive response. The addition of CNT to the initial solution promotes the growth of various PANI–CNT nanostructures, depending on the carbon nanotubes' pretreatment. Thus, nanotubes of ca. 15 μm length are obtained when synthetizing either aniline solution without CNT or with the addition of CNTf. The mean outside diameter is ca. 95 nm (Fig. 1a and c). However, the addition of CNTnf promotes the development of PANI–CNTnf nanoparticles of approximately 90 nm in diameter (Fig. 1b). To explain these facts, it must be taken into account that in the PANI synthesis mechanism, anilinium cations are formed in the first step of the polymerization process [4] and that the CNT chemical pretreatment provokes the formation of carboxyl, hydroxyl and carbonyl groups on their walls [16]. Thus, by incorporating CNTf to the reaction mixture, the negatively charged functional groups of the nanotubes interact with anilinium cations, allowing the adsorption of the CNTf on the walls, hence promoting the growth of polymer chains from them. Other researchers report this type of interaction when using oxidized carbon black and graphene oxide for the synthesis of various polyaniline nanocomposites such as nanotubes, nanospheres and nanofibers [17,18].

In the TEM images of PANI–CNTf structures (Fig. 1f), nanorods of 20–25 nm in diameter and 30–40 nm in length can be distinguished as growing up from the nanotubes walls. Thus, the polymerization process of aniline in dilute SDS/HCl aqueous solution at room temperature lead to the formation of PANI nanostructures covered with submicrotubes. The morphology and size of the PANI structure are influenced by the concentration of surfactant, the added inorganic acid and the temperature [19,20].

When adding CNTnf, the structure of the developed PANI composites adopt a granular morphology formed by nanoparticle aggregates which rarely stayed isolated [4]. In this respect, it is claimed that PANI nanoparticles require a preexisting support (such as nanofibers or nanoribbons) acting as substrate where heterogenous arrangements grew without any preferential direction. Moreover, thermodynamic considerations support the fact of a granular morphology tendency because a spherical cluster possesses a total surface energy

lower than a long chain [17], possibly due to both the low solubility of PANI and the repulsion forces existing between the charges of the polymer chain [21,22].

3.2. FTIR spectra

The identification of existing interactions in the synthesized nanostructures is done by infrared spectroscopy studies. Several bands appear in all the PANI nanostructures spectra (Fig. 2) [4,23–25]. The location of the common bands and the corresponding identification is as follows: 1142 cm^{-1} (assigned as –N=quinoid=N–), 1305 cm^{-1} (CN stretching with aromatic conjugation), 1500 and 1588 cm^{-1} (C=C stretching in benzoides and quinoid rings respectively), 2847 and 2916 cm^{-1} (CH stretching of $-CH_3$ and $-CH_2-$, respectively, which shows the presence of SDS in the synthesized products). As reported in Ref. [22], the anionic surfactant contribute doping the PANI chain via electrostatic interactions with the anilinium cation at the beginning of the polymerization process, and then, forming a supramolecular structure.

In PANI and PANI–CNTf nanostructures spectra, a band at 1042 cm^{-1} is distinguishable; it corresponds to the substitution of S=O groups in the 1,2,4-aromatic rings, indicating a doped PANI structure as a result of using APS during the synthesis. Another band located at 3250 cm^{-1} is assigned to the NH-stretching associated to different of intra- and inter-molecular hydrogen bonds in secondary amines. In the presence of a sulfonate group, a hydrogen bond such as the NH···O type can be proposed. The presence of hydrogen bonds is indicative of a self-organization process of PANI chains in supramolecular assemblies and can be associated to the stabilization of the nanotubes [19,26].

For PANI–CNTf nanostructures, their spectra present two new clear bands, one at 825 cm^{-1} assigned to deformation out of the plane of CH– benzoides rings and the other one at 1248 cm^{-1} corresponding to CN– stretching in secondary aromatic amines [17]. The appearance of these bands indicates that there are interactions between PANI and CNTf in the joint nanostructure.

3.3. UV–vis spectra

UV–vis spectra supply more evidences to elucidate the chemical nature of the prepared nanostructures. PANI nanostructures without added CNT present two adsorption zones in the UV–vis spectra (Fig. 3). One of these bands located in the 294, 360, 436 nm range (possibly overlapping) is related to PANI chain protonation and the other band between 600 and 850 nm is attributed to the π-polaron transition [9,19].

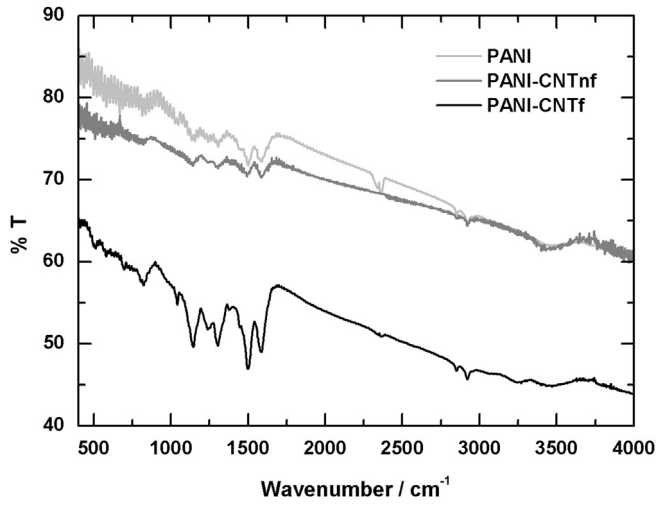

Fig. 2. FTIR spectra of the synthesized nanostructures.

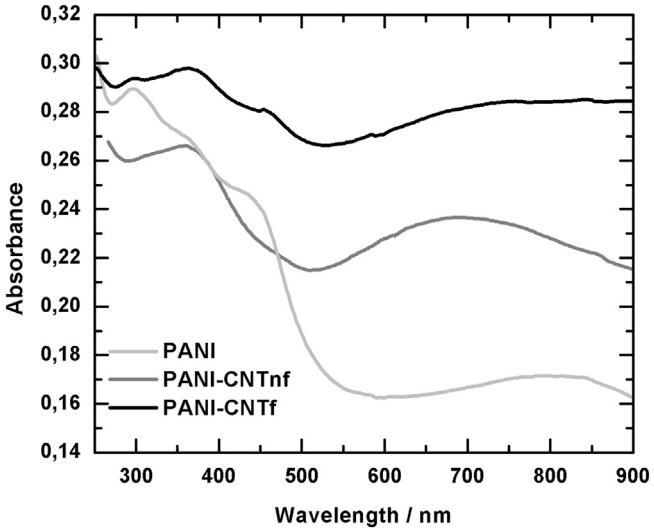

Fig. 3. UV–vis spectra of the synthesized nanostructures.

For PANI–CNTf nanostructures, the spectra show a maximum absorption peak at 360 nm assigned to the π–π* transition in benzoides rings and, then, a broad peak between 600 and 900 nm attributed to a π-polaron transition. Another two shoulders can be observed at 290 and 434 nm related to the mentioned PANI chain protonation, indicating a doped state. Both PANI and PANI–CNTf nanotubes are in the emeraldine salt form which is the conductive PANI form [12,18,19]. The linear nature of the emeraldine chains is responsible to act as pattern to form nanofibers in the early growing steps of the nanostructures [18].

In PANI–CNTnf spectra, two absorption bands at 340 and 676 nm are well defined (Fig. 3); they are attributed to π–π* transitions in quinoid and benzoides rings, respectively, indicating the presence of the emeraldine form, i.e. the non-conductive PANI form [19].

3.4. Cyclic voltammetric studies

Voltamperommetric runs of the prepared nanostructures are carried out between 0.0 V and 1.0 V at various scan rates in order to evaluate their electrochemical characteristics. The typical voltammograms of the nanocomposites are shown in Fig. 4. The anodic and cathodic current peaks assigned to PANI leucoemeraldine/emeraldine pair at ca. 0.4 V are clearly distinguished [12]. At all scan rates, pronounced reversible redox waves are observed in the profiles of PANI–CNTf and PANI–CNTnf electrodes, indicating their better capacitive behavior as compared to PANI electrode. This fact may be due to the combined contributions from both PANI and CNT structures. That is, the synthetized PANI–CNTnf composite provides a large surface area allowing a better electrolyte access as well as providing lower internal resistance [15].

3.5. Galvanostatic charge/discharge experiments

Galvanostatic charge/discharge measurements at different current densities are performed in order to understand the behavior of PANI, PANI–CNTs and PANI–CNTf nanostructures for supercapacitor applications. Typical potential versus time profiles for a constant current density of 2 A g^{-1} are shown in Fig. 5. Other

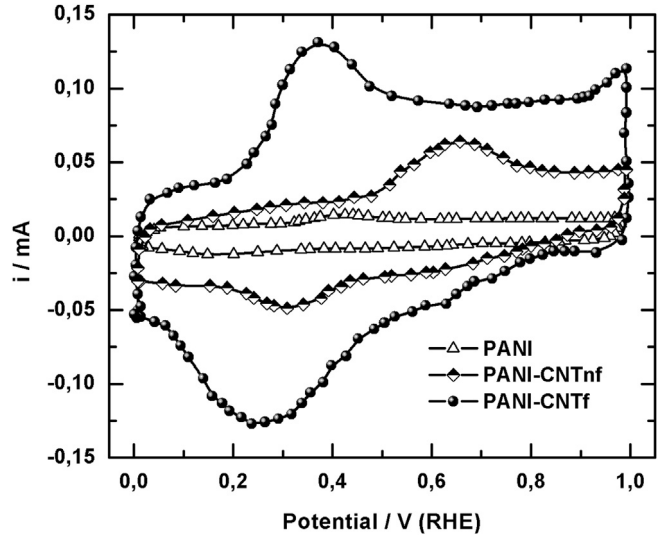

Fig. 4. Cyclic voltammograms of the nanostructured composite electrodes at 20 mV s^{-1} in 0.5 M H_2SO_4.

supercapacitor materials such as activated carbon, metal oxides, carbon nanotubes and carbon blacks exhibit the observed behavior that corresponds to the ideally triangular shaped charging/discharging pattern [8,27,28]. In the present case, the curves are not straight lines indicating the occurrence of a faradaic reaction among the electrode materials. In addition, an initial potential drop can be observed caused by internal resistance [9].

The electrical parameters of the capacitor, namely, specific capacitance (C_m), specific energy (E_s) and specific power (P_s) are calculated using Eqs. (1)–(3).

$$C_m = \frac{C}{m} = \frac{I\Delta t}{\Delta V m} \quad (1)$$

$$E_s = \frac{I\Delta V \Delta t}{m} \quad (2)$$

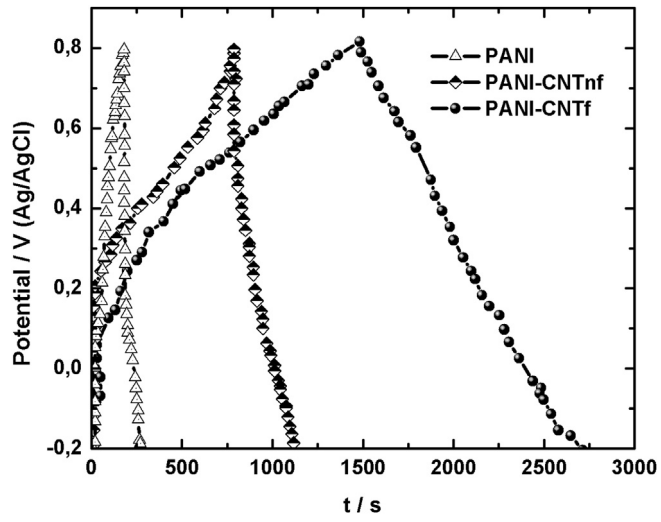

Fig. 5. Galvanostatic charge/discharge curves of the nanostructured composite electrodes for a current density of 2 A g^{-1} in 0.5 M H_2SO_4.

$$P_s = \frac{I\Delta V}{m} \quad (3)$$

where C_m is the specific capacitance, I is the charge/discharge current, Δt is the discharge time, ΔV is the potential range and m is the mass of active material [9,29–31].

The simple self-organization chemical method provokes the formation of unique PANI and PANI/CNTs structures where the total mass and volume are involved in the charge storage and lead to the high SC values. In particular, at 2 A g^{-1}, specific capacitance values of 314, 838 and 1744 F g^{-1} were obtained for pure PANI, PANI–CNTnf and PANI–CNTf nanostructures, respectively (Table 1). It is of interest to compare our results with other SC values reported that involve different PANI and PANI composite dispositions under various experimental conditions. Thus, for PANI nanostructures, the SC values varied from ca. 200 to 2300 F g^{-1} [8,9,32–35]. When considering PANI–CNTs composites, the SC notified values are in the range of 200–606 F g^{-1} [8,15,32,33]. For CNTs, very unlike values are communicated [33,36]. There are also high SC values informed for PANI electrodeposited, i.e. on carbon fiber cloth (1026.8 F g^{-1}), on vertically aligned CNTs (1030 F g^{-1}) on porous carbon rods (1600 F g^{-1}) [24,37,38]. In the case of the outstanding behavior of the PANI–CNTf composites developed by the self-organizing method, several factors can be considered as responsible for the results. In particular, it is to point out the existing charge carriers in these arrays and the fact that the CNTs were pretreated before use. Thus, it was reported that the charge carriers can either move within the polymer structure along the chains or jump from chain to chain by interchain hopping [39]. Moreover, ab-initio calculations showed that quinoid structures present a large affinity for charges which acquire high mobility attributed to the delocalized polarons [40]. Recently, it was proposed that the incorporation of highly conducting CNTs in the PANI matrix increases noticeably the conductivity of the samples because of a strong coupling between the CNTs and the polymer chains [41]. The established interaction is considered as coming from a charge transfer process between the quinoid rings of PANI and the CNTs. On the other hand, the incorporated CNTs contribute to the SC values not only by adding to the double layer capacity due to the facile accessibility of the electrolyte in the internal and external porous structure, but by supplying faradaic pseudo-capacitance generated on the superficial oxygenated groups developed during the acid pretreatment.

Since long cycle-life is a very important parameter to be taken into account when using these materials as electrochemical capacitors, the cycle charge/discharge test is employed to examine the stability of the prepared electrodes for 1000 cycles at 2 A g^{-1}. The specific discharge capacitances of the different electrode materials as a function of the number of cycles are presented in Fig. 6. The capacitance of PANI–CNTf composites is greater than the values corresponding to PANI and PANI–CNTnf nanostructures. The loss of capacitance during the charge/discharge cycles is lower than

Table 1
Specific capacitances of the developed nanomaterials.

I (A g^{-1})	Nanomaterial		
	PANI	PANI–CNTnf	PANI–CNTf
	C_m (F g^{-1})		
2	314	838	1744
4	134	340	1012
10	72	150	490
20	58	60	360
40	42	43	320
100	36	38	262

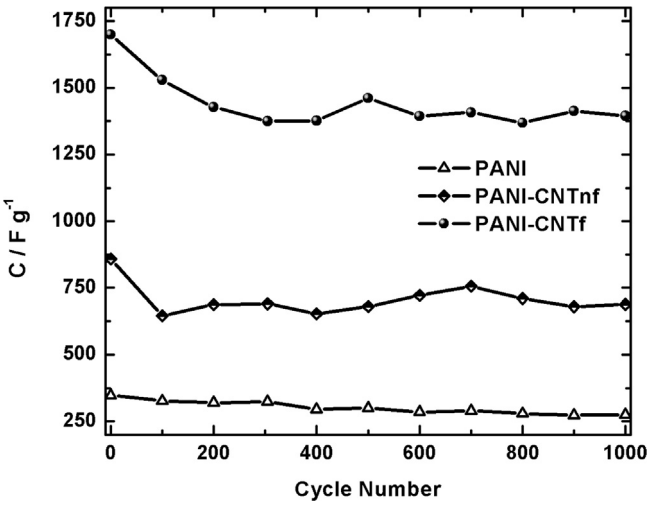

Fig. 6. Cycle-life curves of nanostructured composite electrodes at 2 A g^{-1}.

21% for the three checked materials. These results reveal that the service-life can be improved remarkably when having CNT, either CNTnf or CNTf, in the PANI nanostructures.

An adaptation of the Ragone plot [31] is presented in Fig. 7 showing the relationship between the specific power density and specific energy density for PANI, PANI–CNTf and PANI–CNTnf nanostructures. PANI–CNTf composites show much higher specific power and specific energy values than PANI and PANI–CNTnf structures. For PANI–CNTf composites, a high specific power of 100 kW kg^{-1} and a specific energy of 485 W h kg^{-1} are obtained. It is to point out that for the same specific power value, the specific energy of PANI–CNTf composite electrodes is four times larger than the value corresponding to PANI electrodes.

The better performance is attributed to the singular porous nanostructures, developed by the chemical method, offering a great many charge passways. The morphology of the prepared nanostructures with their characterized chemical interactions that facilitates the charge transport processes and/or the occurrence of faradaic reactions.

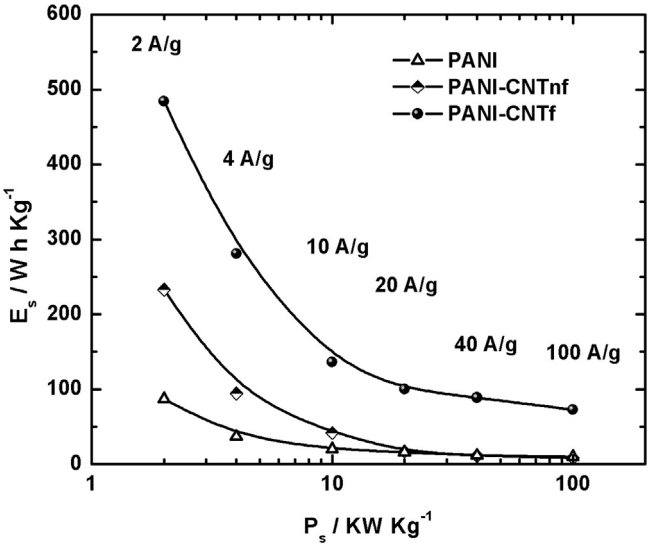

Fig. 7. Relationship between the specific power density and specific energy density of the nanostructured composite electrodes in 0.5 M H_2SO_4.

4. Conclusions

Polyaniline and polyaniline–carbon nanotubes nanostructures were chemically synthesized using a simple method of self-organization. Changes in the molecular structures, in the state of doped PANI during polymerization process and in the stabilization of these links by hydrogen bridge interactions led to different PANI and PANI–CNT nanostructures. Hence, nanotubes with an outer diameter of ca. 95 nm were obtained from acid solutions containing either aniline or the monomer with the addition of functionalized CNT. Their length varied from ca. 10 to 15 microns. When incorporating unfunctionalized CNT to the initial reaction solution, granular aggregates of ca. 95 nm in diameter were produced. The electrochemical characterization of the synthetized nanostructures has been carried out applying voltamperommetric and charge/discharge runs. The experimental capacitance and the service life data indicate that the developed nanostructures can be applied as supercapacitor materials.

Acknowledgments

The authors acknowledge the support of SECAT-Facultad de Ingeniería - UNCPBA and CICPBA.

References

[1] M. Winter, R.J. Brodd, Chem. Rev. 104 (2004) 4245–4269.
[2] Y. Zhang, H. Feng, X. Wu, L. Wang, A. Zhang, T. Xia, H. Dong, X. Li, L. Zhang, Int. J. Hydrogen Energy 34 (2009) 4889–4899.
[3] L. Pan, H. Qiu, Ch. Dou, Y. Li, L. Pu, J. Xu, Y. Shi, Int. J. Mol. Sci. 11 (2010) 2636–2657.
[4] C. Laslau, Z. Zujovic, J. Travas-Sejdic, Prog. Polym. Sci. 35 (2010) 1403–1419.
[5] J.-B. He, Ch.-L. Chen, J.-H. Liu, Sens. Actuators, B 99 (2004) 1–5.
[6] L. Agüí, P. Yáñez-Sedeño, J.M. Pingarrón, Anal. Chim. Acta 622 (2008) 11–47.
[7] A. Guha, W. Lu, T. Zawodzinski, D. Schiraldi, Carbon 45 (2007) 1506–1517.
[8] B. Dong, B.-L. He, C.-L. Xu, H.-L. Li, Mater. Sci. Eng., B 143 (2007) 7–13.
[9] H. Mi, X. Zhang, S. Yang, X. Ye, J. Luo, Mater. Chem. Phys. 112 (2008) 127–131.
[11] P. Chandrasekhar, Conducting Polymers, Fundamentals and Applications. A Practical Approach, Kluwer Academic Publishers, Boston–Dordrecht–London, 1999.
[12] D.E. Stilwell, S.-M. Park, J. Electrochem. Soc. 135 (1988) 2254–2262.
[13] M. Aldissi, Intrinsically Conducting Polymers: An Emerging Technology, North Atlantic Treaty Organization. Scientific Affairs Division, Burlington, Vermont, USA, 1992.
[14] G. Wu, L. Li, J.-H. Li, B.-Q. Xu, Carbon 43 (2005) 2579–2587.
[15] S.R. Sivakkumar, W.J. Kim, J.-A. Choi, D.R. MacFarlane, M. Forsyth, D.-W. Kim, J. Power Sources 171 (2007) 1062–1068.
[16] L. Vaccarini, C. Goze, R. Aznar, V. Micholet, C. Journet, P. Dernier, Synth. Met. 103 (1999) 2492–2493.
[17] K.R. Reddy, B.C. Sin, K.S. Ryu, J. Noh, Y. Lee, Synth. Met. 159 (2009) 1934–1939.
[18] Y.F. Huang, C.W. Lin, Polymer 53 (2012) 2574–2582.
[19] C. Zhou, J. Han, R. Guo, Macromolecules 42 (2009) 1252–1257.
[20] D. Li, R.B. Kaner, J. Am. Chem. Soc. 128 (2006) 968–975.
[21] C. Laslau, Z.D. Zujovic, J. Travas-Sejdic, Macromol. Rapid Commun. 30 (2009) 1663–1668.
[22] S.P. Surwade, N. Manohar, S.K. Manohar, Macromolecules 42 (2009) 1792–1795.
[23] R. Cruz-Silvaa, J. Romero-García, J.L. Angulo-Sánchez, E. Flores-Loyola, M.H. Farías, F.F. Castillón, J.A. Díaz, Polymer 45 (2004) 4711–4717.
[24] H. Zhang, G. Cao, Z. Wang, Y. Yang, Z. Shi, Z. Gu, Electrochem. Commun. 10 (2008) 1056–1059.
[25] L. Nikzad, M.R. Vaezi, B. Yazdani, Int. J. Mod. Phys.: Conf. Ser. 5 (2012) 527–535.
[26] J. Stejskal, I. Sapurina, M. Trchová, E.N. Konyushenko, P. Holler, Polymer 47 (2006) 8253–8262.
[27] A.G. Pandolfo, A.F. Hollenkamp, J. Power Sources 157 (2006) 11–27.
[28] X.-M. Liu, X.-G. Zhang, Sh.-Y. Fu, Mater. Res. Bull. 41 (2006) 620–627.
[29] A. Sumboja, X. Wang, J. Yang, P.S. Lee, Electrochim. Acta 65 (2012) 190–195.
[30] W.-Ch. Chen, T.-Ch. Wen, H. Teng, Electrochim. Acta 48 (2003) 641–649.
[31] V. Gupta, N. Miura, Electrochim. Acta 52 (2006) 1721–1726.
[32] Y. Zhou, B. He, W. Zhou, J. Huang, X. Li, B. Wu, H. Li, Electrochim. Acta 49 (2004) 257–262.
[33] V. Gupta, N. Miura, J. Power Sources 157 (2006) 616–620.
[34] K. Rajendra Prasad, N. Munichandraiah, J. Power Sources 112 (2002) 443–451.

[35] T.C. Girija, M.V. Sangaranarayanan, J. Power Sources 159 (2006) 1519–1526.
[36] Q. Chen, K. Xue, W. Shen, F. Tao, S. Yin, W. Xu, Electrochim. Acta 49 (2004) 4157–4161.
[37] Q. Cheng, J. Tang, J. Ma, H. Zhang, N. Shinya, L. Qin, J. Phys. Chem. C 115 (2011) 23584–23590.
[38] S.K. Mondal, K. Barai, N. Munichandraiah, Electrochim. Acta 52 (2007) 58–64.
[39] J.L. Bredas, G.B. Street, Acc. Chem. Res. 18 (1985) 309–315.
[40] M. Wohlgenannt, X.M. Jiang, Z.V. Vardeny, Phys. Rev. B 69 (2004) 241204(R).
[41] G. Chakraborty, K. Gupta, D. Rana, A.K. Meikap, Adv. Nat. Sci. Nanosci. Nanotechnol. 3 (2012) 035015 (8pp).